The Journal of Antibiotics (2017) 70, 179–186

www.nature.com/ja

ORIGINAL ARTICLE

Vestaines, novel vasoactive compounds, isolated from *Streptomyces* sp. SANK 63697

Yuki Hirota-Takahata[1], Emi Kurosawa[1], Yoko Ishimoto[2], Yuko Iwadate[1], Masaaki Kizuka[1], Jun Chiba[3], Toru Hasegawa[4], Masahiro Tanaka[1] and Hideki Kobayashi[2]

We conducted a screening program for vasoactive compounds and detected a potent activity in the cultured broth of *Streptomyces* sp. SANK 63697. From the cultured broth, two active compounds, vestaine A_1 and B_1, were isolated. The structures of these compounds were elucidated by physicochemical data and spectral analyses, and found to be new compounds.
The Journal of Antibiotics (2017) **70,** 179–186; doi:10.1038/ja.2016.98; published online 17 August 2016

INTRODUCTION

Blood vessels deliver oxygen and nutrition into all the tissues of our body, and collect carbon dioxide and waste products. It is essential to maintain vessels' integrity, thus our body possesses angiogenesis, which is a process critical to forming new vessels. When tissues are damaged, pro-angiogenic factors stimulate the regeneration of new vessels, and such newly formed vessels are stabilized by means of tightening cell–cell junctions, being covered with mural cells, lined with extracellular matrix and so on.[1] However, excess angiogenesis induces fragile and leaky blood vessel formation, and causes several pathological conditions.[2,3]

Vascular endothelial growth factor (VEGF) is a key molecule of both angiogenesis and endothelial permeability.[4] Excess angiogenesis and increased permeability induced by overproduction of VEGF are observed in patients suffering from several diseases, such as retinopathy and cerebral hemorrhage.[5,6] This indicates that vasoactive substances, which not only assist angiogenesis, but also cancel the adverse effects of VEGF, are useful for treating diseases caused by fragile and leaky vessels. To evaluate vasoactive effect, the VS-G assay, a co-culture system of endothelial cells with fibroblasts, had been established.[7] In the course of screening to obtain vasoactive compounds, the morphological changes of human umbilical vein endothelial cells (HUVECs) were used as an indicator of candidate compounds in the VS-G assay. Potent activity was detected in the cultured broth of *Streptomyces* sp. SANK 63697, and two active compounds named vestaine A_1 (**1**) and B_1 (**2**) were isolated, and their structures were elucidated (Figure 1).

In this report, we describe the taxonomy of the producing organism, isolation, physicochemical properties and structural elucidations of vestaines. Details of the biological activities will be reported independently.[7]

RESULTS

Taxonomy of the producing organism

The strain SANK 63697 was isolated from a leaf of *Terminalia catappa* collected in Tokyo, Japan. The strain grew well on yeast extract–malt extract agar (ISP 2) and inorganic salts–starch agar (ISP 4), and the colony color was pale yellow to brown. The mass of aerial mycelia produced on ISP 2, oatmeal agar (ISP 3), ISP 4, glycerol–asparagine agar (ISP 5) and tyrosine agar (ISP 7) was white to gray. The mature spore chains were rectinaculiaperti and each had >20 spores per chain. The spores had a smooth surface (Figure 2).

The 16S ribosomal RNA gene sequence (1472 nucleotides) was determined and analyzed using the EzTaxon-e database.[8] The results indicated that the gene sequences between SANK 63697 and *Streptomyces tendae* ATCC 19812^T (D63873) showed a 100.0% similarity. On the basis of the morphological and cultural properties, and 16S ribosomal RNA gene sequence similarity, the strain SANK 63697 was classified into *Streptomyces* sp. SANK 63697 (Figure 2).

Isolation

The cultured broth (5 l) was filtered with the assistance of Celite 545 (Thermo Fisher Scientific, Waltham, MA, USA) and separated into mycelium and supernatant. The active substances were extracted from the mycelium with 80% aq. acetone (1.2 l) and the extract was filtered as described above. After addition of *n*-butanol (100 ml) as a defoaming agent, the filtrate was concentrated *in vacuo* to remove acetone. The pH of the concentrate was adjusted to 3.0 with 1 N HCl and then the concentrate was subjected to a Diaion HP-20 column (Mitsubishi Chemical, Tokyo, Japan, 200 ml). The column was washed with 30% aq. acetone (600 ml) and the active substances were eluted with 80% aq. acetone (600 ml). The eluate was concentrated *in vacuo* to dryness to give an oily substance (418 mg).

[1]Discovery Science and Technology Department, Daiichi Sankyo RD Novare, Tokyo, Japan; [2]Frontier Research Laboratories, Daiichi Sankyo, Tokyo, Japan; [3]Medicinal Chemistry Research Laboratories, Daiichi Sankyo, Tokyo, Japan and [4]Organic Synthesis Department, Daiichi Sankyo RD Novare, Tokyo, Japan
Correspondence: Dr H Kobayashi, Frontier Research Laboratories, Group IV, Daiichi Sankyo, 1-2-58 Hiromachi, Shinagawa-ku, Tokyo 140-8710 Japan.
E-mail: kobayashi.hideki.gc@daiichisankyo.co.jp
Received 12 May 2016; revised 24 June 2016; accepted 7 July 2016; published online 17 August 2016

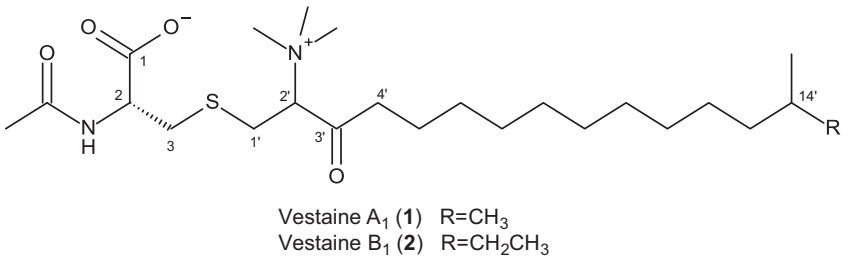

Figure 1 Structures of vestaines.

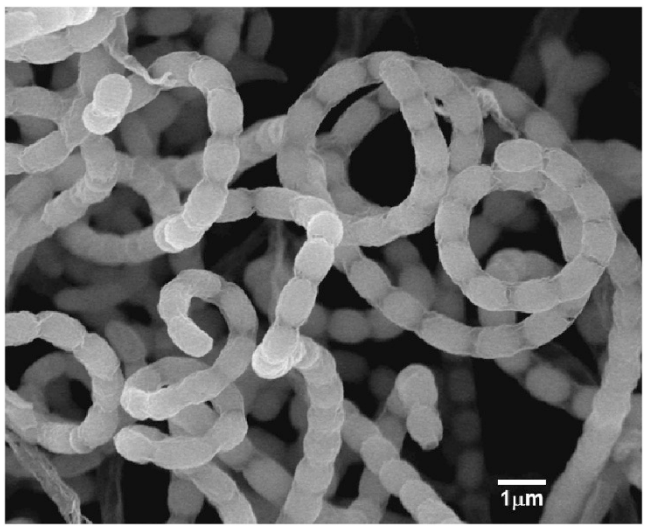

Figure 2 Scanning electron micrograph of strain SANK 63697 grown on ISP 4 for 2 weeks at 28 °C.

The substance was dissolved in 20 ml of 50% aq. ethanol and was subjected to an ODS open column (Cosmosil 140C18-OPN, Nacalai Tesque, Kyoto, Japan, 40 ml). The chromatography was performed by a stepwise elution using 40, 45 and 50% MeCN in 0.1 M aq. $NaClO_4$ (200, 800 and 400 ml, respectively). These eluates were fractionated into 15 ml portions.

*Isolation of vestaine A_1 (**1**).* Fractions of the 45% MeCN in 0.1 M aq. $NaClO_4$ eluate containing **1** in the Cosmosil column chromatography were combined and concentrated *in vacuo* to remove MeCN. For desalting, the residue was subjected to an HP-20 column (10 ml). After washing the column with water (40 ml), **1** was eluted with 80% aq. acetone (40 ml). The eluate was concentrated *in vacuo* to dryness to give a partially purified substance (24.1 mg). The substance was further purified by preparative HPLC using an ODS column (SYMMETRY C18, 19 i.d. × 100 mm, Waters, Milford, MA, USA). The chromatography was performed with MeCN/0.05 M $NaClO_4$ (45:55) at a flow rate of 9 ml min^{-1}. The eluate containing **1** was concentrated and subsequently desalted in the same manner as described above, and concentrated *in vacuo* to dryness to give **1** as a white powder (12.2 mg).

As a result of HPLC analysis, **1** was exhibited as two peaks (peak 1 and peak 2) with the same molecular formula shown in Figure 3.

*Isolation of vestaine B_1 (**2**).* Fractions of the 45–50% MeCN in 0.1 M aq. $NaClO_4$ eluate containing **2** on the Cosmosil column chromatography were combined and concentrated *in vacuo* to remove MeCN. For desalting, it was subjected to an HP-20 column (20 ml). After washing the column with water (80 ml), **2** was eluted with 80% aq. acetone (80 ml). The eluate was concentrated *in vacuo* to dryness to give a partially purified substance (50.6 mg). The substance was applied to the preparative HPLC using the same ODS column described above. The chromatography was performed with MeCN/0.05 M $NaClO_4$ (50:50) at a flow rate of 9 ml min^{-1}. The eluate containing **2** was concentrated. It was then desalted as described above and concentrated *in vacuo* to dryness to give a substance mainly containing **2** (23.7 mg). Finally, it was rechromatographed by the same preparative HPLC using the solvent system of MeCN/0.05 M $NaClO_4$ (45:55), desalted in the same manner as above and concentrated *in vacuo* to dryness to give pure **2** as a white powder (12.7 mg). **2** also gave two peaks (peak 3 and peak 4) in the analytical HPLC.

Physicochemical properties

Physicochemical properties of the vestaines are summarized in Table 1. The molecular formula of each compound was determined by positive ion ESIMS. Peaks 1 and 2 showed the same molecular formula of $C_{24}H_{46}N_2O_4S$, and peaks 3 and 4 also have the same as that of $C_{25}H_{48}N_2O_4S$. The presence of a sulfur atom was further proved by two characteristic isotopic ions at 461.3211 ($C_{24}H_{47}N_2O_4{}^{34}S$) and 461.3297 ($C_{22}{}^{13}C_2H_{47}N_2O_4S$) for **1** as shown in Figure 3d, and at 475.3368 ($C_{25}H_{49}N_2O_4{}^{34}S$) and 475.3455 ($C_{23}{}^{13}C_2H_{49}N_2O_4S$) for **2**.

Structural elucidation

*Structural elucidation of vestaine A_1 (**1**).* The structural elucidation was mainly focused on **1**. The ^1H and ^{13}C NMR spectral data obtained in methanol-d_4 are summarized in Table 2. As well as the HPLC pattern of **1**, a pair of signals was observed in the NMR spectra. Therefore, observed NMR signals of **1** were classified into two categories as **1a** and **1b**.

In the ^1H NMR signal set of **1a**, signals from the highly overlapped alkyl group (δ 1.22–1.39), including three methyl groups were observed. In addition, two signals (δ 2.80–2.90 and 4.6) disappeared over time. It seemed to indicate that this phenomena was observed in the process when **1b** was formed from **1a** or vice versa, and it was dependent on tautomerism. In the ^{13}C NMR spectrum, 16 assignable signals and some overlapped signals (δ 53.2 and 30.6–30.8) were observed. As the latter of the overlapped signals (δ 30.6–30.8) were all methylene carbon signals, it was suggested that **1a** included an alkyl chain moiety. The observed 16 assignable signals were classified into 3 × methyl, 7 × methylene, 3 × methine and three quaternary carbons by DEPT spectrum. Two carbon signals that became hard to observe existed as well as the proton signals (C-2′ and C-4′).

Three partial structures as shown in Figure 4a were elucidated by several NMR techniques, such as DQF-COSY, HSQC, HMBC and ^1H–^{15}N HMBC. In addition, an alkyl chain that had the partial structure of (c) as a terminal was recognized. Although there was no direct evidence of a sulfur atom-binding position, the appropriate position was between C-3 and C-1′, because of the chemical shift value

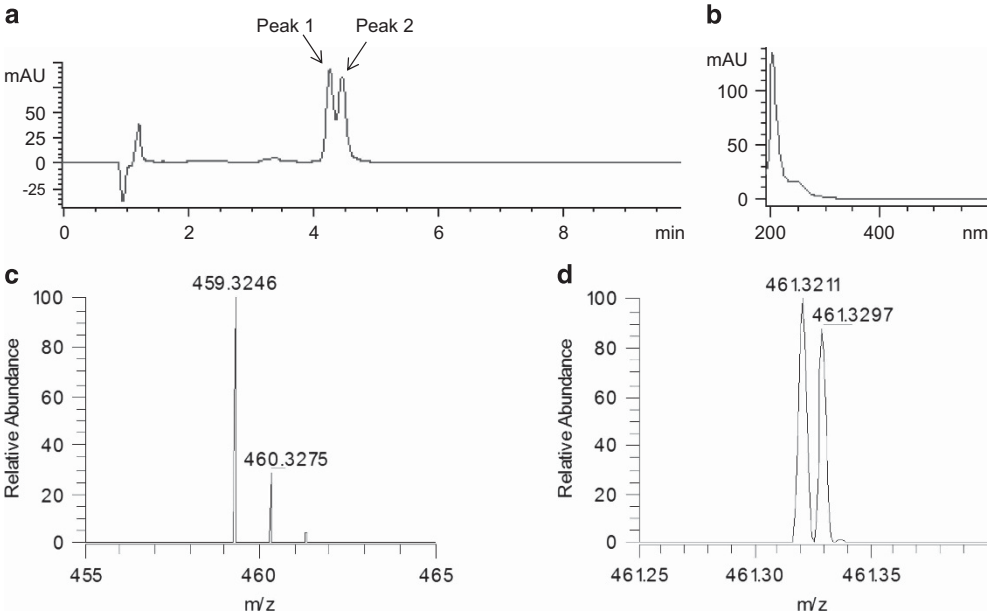

Figure 3 HPLC and HR-MS data (ESI) of **1**. (**a**) HPLC chart of **1**. HPLC conditions: column, Unison UK-C18, 3 μm, 4.6 i.d.×75 mm; mobile phase, MeCN/20 mM aq. ammonium acetate (1/1); flow rate, 1 ml min^{-1}; sample, 2 mg ml^{-1}, 3 μl injection. (**b**) UV spectrum of peak 1. Both peak 1 and peak 2 show the same UV spectrum. (**c**) HR-MS data (ESI) of peak 1. (**d**) Enlarged view of (**c**) ranged from *m/z* 461.25 to 461.40.

Table 1 Physicochemical properties of vestaine A_1 and B_1

	*Vestaine A_1 (**1**)*		*Vestaine B_1 (**2**)*	
	Peak 1	*Peak 2*	*Peak 3*	*Peak 4*
Appearance	White powder		White powder	
IR ν_{max} cm^{-1} (ATR)	3262, 2923, 2852, 1721, 1654, 1599, 1490, 1467, 1373		3258, 2924, 2853, 1721, 1655, 1601, 1491, 1464, 1375	
Molecular formula	$C_{24}H_{46}N_2O_4S$	$C_{24}H_{46}N_2O_4S$	$C_{25}H_{48}N_2O_4S$	$C_{25}H_{48}N_2O_4S$
HR-MS (m/z)				
Found	459.3246 $(M+H)^+$	459.3244 $(M+H)^+$	473.3400 $(M+H)^+$	473.3400 $(M+H)^+$
Calculated	459.3251 (for $C_{24}H_{47}N_2O_4S$)	459.3251 (for $C_{24}H_{47}N_2O_4S$)	473.3407 (for $C_{25}H_{49}N_2O_4S$)	473.3407 (for $C_{25}H_{49}N_2O_4S$)

Abbreviations: ATR, attenuated total reflection.

of H-3 (δ 2.86 and 3.28) and H-1′ (δ 3.02 and 3.30), and the observed ^1H–^{13}C long-range coupling from H-3 to C-1′ and H-1′ to C-3 without having ^1H–^1H coupling between H-1′ and H-3. It was also supported by the product ion (*m/z* 162) in the collision-induced dissociation spectra of **1**, as shown in Figure 4b. Accordingly, the partial structure (a) was clarified as acetylated cysteine residue. The position of an alkyl chain was axiomatically determined to be between C-3′ of the partial structure (b) and C-11′ of (c). However, the length of the alkyl chain and the number of methyl groups binding to N-2′ remained uncertain.

To elucidate the two unclear points, **1** was dissolved in dimethylsulfoxide-d_6 (DMSO-d_6) and analyzed by several NMR techniques. As a result, it was recognized that **1** was converted to compound **3** in the DMSO-d_6. Compound **3** no longer had tautomerism, and all the carbon signals, including the alkyl chain carbons, were observed clearly. The molecular formula of **3** was determined to be $C_{21}H_{37}NO_4S$ (*m/z*, found 400.2508 $(M+H)^+$, calcd 400.2516 for $C_{21}H_{38}NO_4S$), which is the de-trimethylamine derivative of **1**. By several NMR techniques, the structure of **3** was elucidated and found to be the compound from which N-2′ was eliminated and a new olefin was formed instead, as shown in Figure 5. The results indicated that **1** originally had a trimethylamine group and the Hofmann elimination afforded **3** in DMSO. Thus, the planar structure of **1a** was deductively revealed as shown in Figure 1.

By analyzing all NMR signals derived from the set of **1b**, it was proved to have the same partial structures; therefore, the planar structure of **1b** was determined to be the same as that of **1a**. Namely, **1b** was a diastereomer of **1a** at C-2′ generated through the keto–enol equilibrium.

Stereochemistry of the cysteine residue of **1** was determined by the advanced Marfey's method.[9] Acid hydrolysates of **1** were coupled with L- or D-FDLA (1-fluoro-2,4-dinitorophenyl-5-leucine amide) and analyzed by LC–HR-MS. Almost all DLA-derived cysteine was observed as DLA-derived cystine. By comparing authentic standards, the chirality of cysteine was determined to be L configuration.

*Structural elucidation of vestaine B_1 (**2**).* Compound **2** was also comprised of two forms: **2a** and **2b**, it is uncertain which peak observed in the HPLC analysis is **2a**/**2b**. As shown in Table 1, the molecular formulae of **2a** and **2b** had one more methylene than those

Table 2 ^{1}H and ^{13}C NMR signal assignments of vestaines in methanol-d_4

	*Vestaine A_1 (**1**)*					
	1a			***1b***		
	δ_C	δ_H		δ_C	δ_H	
	After deuteration	*Before deuteration*	*After deuteration*	*After deuteration*	*Before deuteration*	*After deuteration*
N-*acetyl Cys*						
1	176.3 (s)			176.3 (s)		
2	55.0[a] (d)	4.43 (1H, dd, 4.7, 7.0 Hz)	4.43 (1H, dd, 4.7, 7.0 Hz)	55.1[a] (d)	4.45 (1H, dd, 4.7, 6.0 Hz)	4.45 (1H, dd, 4.7, 6.0 Hz)
3	36.9 (t)	2.80–2.90 (1H, *)	2.86 (1H, dd, 7.0, 14.2 Hz)	36.1 (t)	2.93–3.06 (1H, *)	3.02 (1H, dd, 6.0, 14.2 Hz)
		3.27 (1H, *)	3.28 (1H, *)		3.10 (1H, dd, 4.7, 14.2 Hz)	3.10 (1H, dd, 4.7, 14.2 Hz)
2-NHAc	172.8[b] (s)			172.9[b] (s)		
	22.8 (q)	2.01 (3H, s)	2.01 (3H, s)	22.9 (q)	2.02 (3H, s)	2.02 (3H, s)
Alkyl chain						
1′	28.8 (t)	2.93–3.06 (1H, *)	3.02 (1H, d, 13.5 Hz)	28.5 (t)	2.93–3.06 (1H, *)	2.97 (1H, d, 13.5 Hz)
		3.31 (1H, *)	3.30 (1H, *)		3.37 (1H, dd, 3.7, 13.5 Hz)	3.37 (1H, d, 13.5 Hz)
2′	75.5 (d)	4.58 (*, dd, 3.6, 10.9 Hz) [c]	Disappeared	75.7 (d)	4.60 (*, dd, 3.6, 10.9 Hz) [c]	Disappeared
3′	207.2 (s)			207.2 (s)		
4′[d]		2.80–2.90 (*, *)	Disappeared		2.80–2.90 (*, *)	Disappeared
5′	23.6 (t)	1.57–1.67 (2H, m)	1.57–1.65 (2H, m)	23.6 (t)	1.57–1.67 (2H, m)	1.57–1.65 (2H, m)
6′	29.8[e] (t)			29.8[f] (t)		
7′	30.57[e] (t)			30.57[f] (t)		
8′	30.61[e] (t)			30.61[f] (t)		
9′	30.75[e] (t)	1.22–1.39 (14H, *)	1.22–1.39 (14H, *)	30.75[f] (t)	1.22–1.39 (14H, *)	1.22–1.39 (14H, *)
10′	30.83[e] (t)			30.83[f] (t)		
11′	31.1 (t)			31.1 (t)		
12′	28.5 (t)			28.5 (t)		
13′	40.3 (t)	1.14–1.20 (2H, m)	1.14–1.20 (2H, m)	40.3 (t)	1.14–1.20 (2H, m)	1.14–1.20 (2H, m)
14′	29.2 (d)	1.47–1.57 (1H, m)	1.47–1.57 (1H, m)	29.2 (d)	1.47–1.57 (1H, m)	1.47–1.57 (1H, m)
15′	23.1 (q)	0.88 (3H, d, 6.7 Hz)	0.88 (3H, d, 6.7 Hz)	23.1 (q)	0.88 (3H, d, 6.7 Hz)	0.88 (3H, d, 6.7 Hz)
2′-N(CH_3)$_3$	53.2 (q)			53.2 (q)		
	53.2 (q)	3.216 (*, s)[g]	3.21 (*, s)[h]	53.2 (q)	3.220 (*, s)[g]	3.22 (*, s)[h]
	53.2 (q)			53.2 (q)		
14′-CH_3	23.1 (q)	0.88 (3H, d, 6.7 Hz)	0.88 (3H, d, 6.7 Hz)	23.1 (q)	0.88 (3H, d, 6.7 Hz)	0.88 (3H, d, 6.7 Hz)

Table 2 Continued

	*Vestaine B_1 (**2**)*					
	2a			***2b***		
	δ_C	δ_H		δ_C	δ_H	
	After deuteration	*Before deuteration*	*After deuteration*	*After deuteration*	*Before deuteration*	*After deuteration*
N-*acetyl Cys*						
1	176.4 (s)			176.4 (s)		
2	55.1 (d)	4.42 (1H, dd, 4.4, 7.0 Hz)	4.42 (1H, dd, 4.4, 7.0 Hz)	55.2 (d)	4.45 (1H, dd, 5.0, 6.1 Hz)	4.45 (1H, dd, 5.0, 6.1 Hz)
3	37.0 (t)	2.80–2.92 (1H, *) 3.28 (1H, *)	2.85 (1H, dd, 7.0, 14.1 Hz) 3.28 (1H, *)	36.1 (t)	2.94–3.06 (1H, *) 3.10 (1H, dd, 5.0, 14.3 Hz)	3.02 (1H, dd, 6.1, 14.3 Hz) 3.10 (1H, dd, 5.0, 14.3 Hz)
2-NHAc	172.8[i] (s)			172.9[i] (s)		
	22.9 (q)	2.01 (3H, s)	2.01 (3H, s)	22.9 (q)	2.02 (3H, s)	2.02 (3H, s)
Alkyl chain						
1′	28.7 (t)	2.94–3.06 (1H, *) 3.28 (1H, *)	3.01 (1H, d, 12.3 Hz) 3.28 (1H, *)	28.5 (t)	2.94–3.06 (1H, *) 3.37 (1H, d, 13.5 Hz)	2.97 (1H, d, 13.4 Hz) 3.37 (1H, d, 13.4 Hz)
2′	75.5 (d)	4.58 (*, dd, 3.6, 10.9 Hz)[j]	Disappeared	75.7 (d)	4.62 (*, dd, 3.6, 10.9 Hz)[j]	Disappeared
3′	207.2[k] (s)			207.3[k] (s)		
4′[l]		2.80–2.92 (*, *)	Disappeared		2.80–2.92 (*, *)	Disappeared
5′	23.6 (t)	1.57–1.69 (2H, m)	1.57–1.69 (2H, m)	23.6 (t)	1.57–1.69 (2H, m)	1.57–1.69 (2H, m)
6′	29.8 (t)			29.8 (t)		
7′	28.2[m] (t)			28.2[n] (t)		
8′	30.6[m] (t)			30.6[n] (t)		
9′	30.6[m] (t)	1.22–1.39 (14H, *)	1.22–1.39 (14H, *)	30.6[n] (t)	1.22–1.39 (14H, *)	1.22–1.39 (14H, *)
10′	30.8[m] (t)			30.8[n] (t)		
11′	30.8[m] (t)			30.8[n] (t)		
12′	31.1[m] (t)			31.1[n] (t)		
13′	37.8 (t)	1.05–1.16 (1H, m) 1.31 (1H, *)	1.05–1.16 (1H, m) 1.31 (1H, *)	37.8 (t)	1.05–1.16 (1H, m) 1.31 (1H, *)	1.05–1.16 (1H, m) 1.31 (1H, m)
14′	35.7 (d)	1.30 (1H, *)	1.30 (1H, *)	35.7 (d)	1.30 (1H, *)	1.30 (1H, *)
15′	30.6 (t)	1.09–1.19 (1H, m) 1.35 (1H, *)	1.09–1.19 (1H, m) 1.35 (1H, *)	30.6 (t)	1.09–1.19 (1H, m) 1.35 (1H, *)	1.09–1.19 (1H, m) 1.35 (1H, *)
16′	11.8 (q)	0.87 (3H, t, 7.2 Hz)	0.87 (3H, t, 7.2 Hz)	11.8 (q)	0.87 (3H, t, 7.2 Hz)	0.87 (3H, t, 7.2 Hz)
2′-N(CH_3)$_3$	53.1[o] (q)			53.2[o] (q)		
	53.1[o] (q)	3.21 (*, s)[p]	3.21 (*, s)[q]	53.2[o] (q)	3.22 (*, s)[p]	3.22 (*, s)[q]
	53.1[o] (q)			53.2[o] (q)		
14′-CH_3	19.7 (q)	0.86 (3H, d, 6.6 Hz)	0.86 (3H, d, 6.4 Hz)	19.7 (q)	0.86 (3H, d, 6.6 Hz)	0.86 (3H, d, 6.4 Hz)

Chemical shifts are given in p.p.m. referenced to tetramethylsilane (TMS).
The measurement that is immediate after dissolution.
*Not clearly observed owing to the overlap.
a–c, g–k and o–q denote changeable; d and l denote not clearly observed owing to the overlap and deuteration; e, f, m and n denote interchangeable.

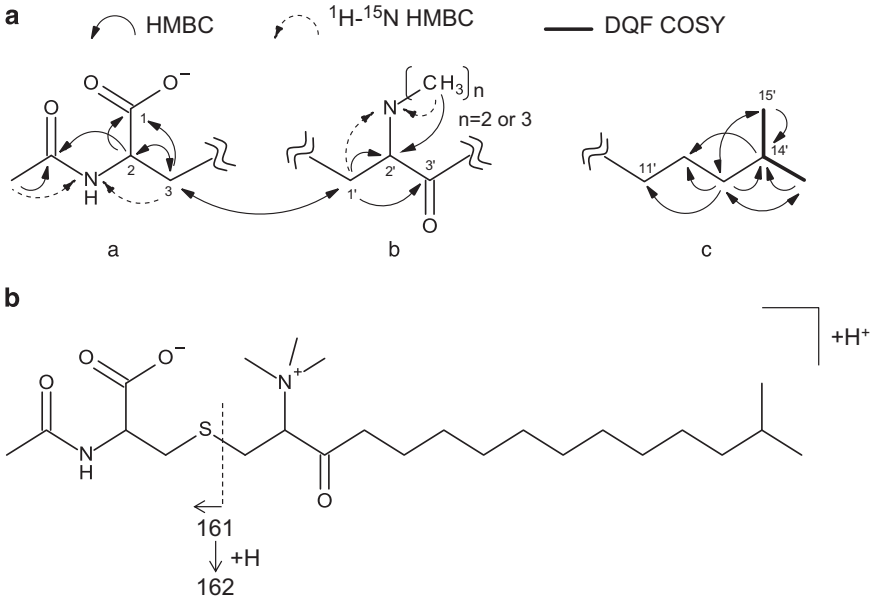

Figure 4 NMR and MS analyses of **1**. (**a**) Partial structures obtained from the NMR analyses of **1**. Both **1a** and **1b** had the same partial structures. (**b**) Product ion observed in coliision-induced dissociation spectra of the protonated molecules of **1**. Both **1a** and **1b** gave the same production.

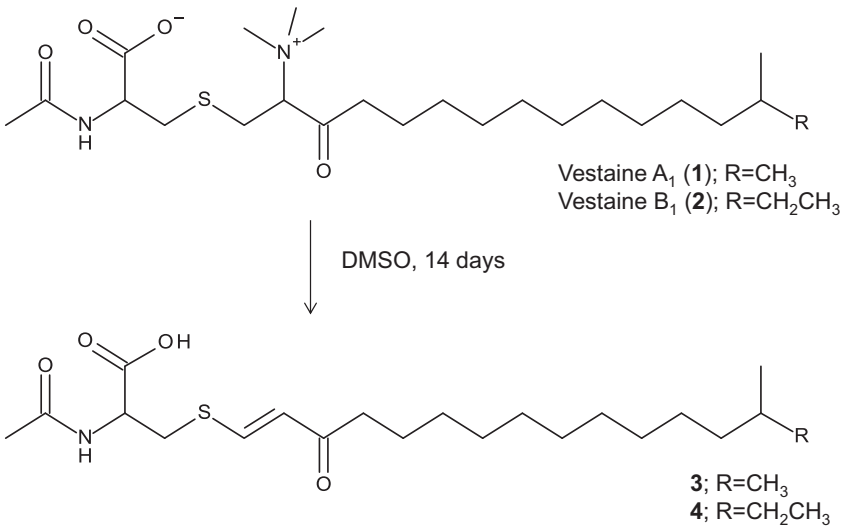

Figure 5 Hofmann elimination of vestaines. DMSO, dimethylsulfoxide.

of **1a** and **1b**. Together with the IR spectral data, the chemical shifts of ^{1}H and ^{13}C NMR signals of **2** in methanol-d_4 (Table 2) were closely similar to those of **1**. Therefore, the structural elucidation of **2** was carried out in the same way as **1**, including the usage of the Hofmann elimination product of **2** (**4**). As a result, **2** was proved to have seco-type endo-terminal as shown in Figure 1.

Biological activities

Both **1** and **2** dose-dependently induced island-shaped morphological changes in the VS-G assay as shown in Figure 6. They showed approximately equal activity. Vestaines induced island-shaped morphology, whereas VEGF induced tube-like morphology in HUVECs. Details of the biological activity of vestaines will be reported independently.[7]

DISCUSSION

In the course of our screening program for vasoactive compounds, two active compounds, vestaine A_1 and B_1, were isolated from the cultured broth of *Streptomyces* sp. SANK 63697. Structures of these were elucidated by physicochemical data and spectral analyses, and they were determined to be new amphoteric compounds. Vestaine A_2, which showed the same molecular formula as A_1, and vestaine B_2, which had the same formula as that of B_1, were also observed in the same cultured broth. As the production of A_2 and B_2 was low, they were not purified.

Vestaines had two typical properties. One is that vestaine A_1 and B_1 both formed two diastereomers through keto–enol equilibrium. The other is that they were unstable under a basic condition. For these properties, we had to devise a method for their purification and structural elucidation.

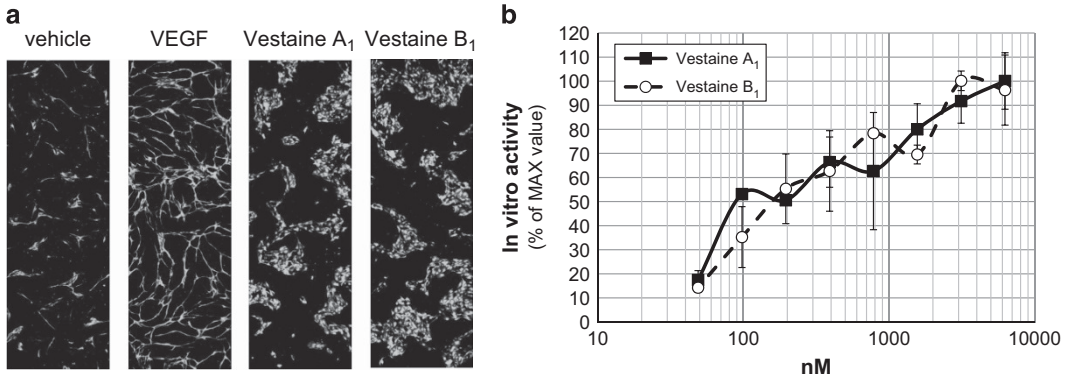

Figure 6 Activities of vestaines in the VS-G assay. (**a**) Morphologies of GFP-HUVECs treated with DMSO, VEGF (50 ng ml^{-1}), vestaine A_1 (195 nM) or vestaine B_1 (195 nM). (**b**) GFP-HUVECs were treated at various concentrations of vestaine A_1 or vestaine B_1. The value of treatment with vestaine A_1 is the black line and that of vestaine B_1 is the dotted line. *In vitro* activity was shown using the number of maximum area value of treatment with vestaine A_1 as a base of 100. Each value is represented as the mean ± range ($n=2$ wells per group). DMSO, dimethylsulfoxide; HUVEC, human umbilical vein endothelial cell; VEGF, vascular endothelial growth factor. A full color version of this figure is available at *The Journal of Antibiotics* journal online.

In the purification, we added sodium perchlorate ($NaClO_4$) to the HPLC mobile phase. $NaClO_4$ is a well-used ion-pairing reagent for HPLC analysis of anion surfactants, and among the solvents we tested, this combination gave a good separation not only for vestaines as the amphoteric surfactants, but also for the two diastereomers of each vestaine.

In the structural elucidation, we could classify all the NMR signals into two sets for each diastereomer, although the signal disappearances caused by hydrogen-deuterium exchange existed. Finally, following the structural elucidation studies of the decomposition products, we deduced the structures of the vestaines. To form such decomposition products in DMSO was also one of the characteristic properties of vestaines. We hypothesized that the Hofmann elimination of vestaines is caused by the basicity of trimethylamine eliminated from the vestaines.

In the stereochemistry determination study of the cysteine residue, we applied the advanced Marfey's method.[9] Although cysteine residue is known to be racemized easily during acid hydrolysis,[10] we expected it would be hard to racemize in the case of vestaines, because the cysteine residue of the vestaines was S-alkylated. This hypothesis was strongly supported by Jacobson *et al.*[11] By using flash hydrolysis techniques,[12] to prevent excess racemization, we obtained the non-racemized cysteine residue and succeeded at determining the chiral configuration of cysteine as being L-form.

In conclusion, the present study revealed that vestaines are novel compounds that possess unique structures and characteristic biological activities. Although VEGF induced tube-like morphology in the VS-G assay, vestaines induced island-shaped morphological changes in HUVECs at a low concentration, which indicates that vestaines affect endothelial cells in a different manner from VEGF. Although it is necessary to analyze their function and mode of action in more detail, vestaines and their derivatives can be unprecedented, useful molecular probes for investigating the mechanism of angiogenesis.

EXPERIMENTAL PROCEDURES

Fermentation

The growth of *Streptomyces* sp. SANK 63697 on an agar slant was homogenized with 10% glycerin (10 ml) and filtered by a cell strainer (mesh size 100 μm, Thermo Fisher Scientific). A portion of the obtained filtrate (50 μl) was transferred into a 500 ml Erlenmeyer flask containing 80 ml of sterilized primary seed medium composed of soluble starch 4.0%, glucose 1.0%, soybean meal 1.0%, yeast extract 0.45%, corn steep liquor 0.25%, $CoCl_2$•$6H_2O$ 0.0001%, KH_2PO_4 0.05%, $ZnSO_4$•$7H_2O$ 0.001%, $Mg_3(PO_4)_2$•$8H_2O$ 0.005%, $NiSO_4$•$6H_2O$ 0.0001% and Disfoam CB-442 (NOF, Tokyo, Japan) 0.005%. The flask was incubated at 28 °C for 48 h on a rotary shaker at 210 r.p.m. The primary seed culture (1 ml) was transferred into a 500 ml Erlenmeyer flask containing 80 ml of sterilized production medium, which was composed of soluble starch 8.0%, glucose 1.0%, soybean meal 1.0%, yeast extract 0.45%, corn steep liquor 0.25% and Disfoam CB-442 0.005%. Each of the 70 flasks were prepared in this way and incubated at 28 °C for 96 h on a rotary shaker at 210 r.p.m.

HPLC analysis of vestaines

Both **1** and **2** are shown as two peaks in the analytical HPLC, respectively. The HPLC conditions are described as follows: column, Unison UK-C18, 3μm, 4.6 i.d. × 75 mm (Imtakt, Kyoto, Japan); mobile phase, MeCN/20 mM aq. ammonium acetate (1:1); flow rate, 1.0 ml min^{-1}. Retention time of each compounds are as follows: peak 1 of **1**, 4.2 min; peak 2 of **1**, 4.4 min; peak 3 of **2**, 5.9 min; peak 4 of **2**, 6.2 min.

General experimental procedures

IR spectra were obtained on an FT/IR-6100typeA spectrometer (JASCO, Tokyo, Japan). NMR spectra were recorded on AVC500 spectrometers equipped with DCH and TCI cryogenic probes (Bruker, Billerica, MA, USA). HR-MS were recorded on an LTQ Orbitrap XL spectrometer (Thermo Fisher Scientific) connected with an Agilent 1200 HPLC System (Agilent Technologies, Santa Clara, CA, USA).

N-acetyl-*S*-[(1*E*)-14-methyl-3-oxopentadec-1-en-1-yl]-L-cysteine (3)

Compound **1** (1.1 mg) was dissolved in DMSO-d_6 and the progress of the reaction was monitored by NMR at fixed intervals. The Hofmann elimination reaction completed for ~14 days and most of **1** was converted into **3**. After analyzed by NMR, the solution was lyophiled and analyzed by LC–HR-MS. HR-MS (ESI): *m/z*: calcd for $C_{21}H_{38}NO_4S$: 400.2516, found: 400.2508 $(M+H)^+$. ^1H NMR (500 MHz, DMSO-d_6, TMS (internal standard)): δ 0.84 (6H, d, $J=6.6$ Hz), 1.10–1.15 (2H, m), 1.19–1.27 (14H, overlapped), 1.43–1.50 (2H, m), 1.47–1.54 (1H, m), 1.83 (3H, s), 2.47 (2H, t, $J=7.3$ Hz), 3.13 (1H, dd, $J=7.1$, 13.2 Hz), 3.31 (1H, dd, $J=4.7$, 13.2 Hz), 4.23 (1H, m), 6.17 (1H, d, $J=15.5$ Hz), 7.75 (1H, d, $J=15.5$ Hz). ^{13}C NMR (125 MHz, DMSO-d_6, TMS (internal standard)): δ 22.4 (two carbons), 22.5, 23.9, 26.7, 27.3, 28.6, 28.7, 28.82, 28.88, 28.95, 29.2, 34.3, 38.4, 39.2*, 52.5, 122.7, 147.0, 168.9, 171.1, 196.1 (*signal was detected by DEPT spectra owing to the overlap with the solvent signals).

N-acetyl-*S*-[(1*E*)-14-methyl-3-oxohexadec-1-en-1-yl]-L-cysteine (4)

Compound **2** (1.2 mg) was dissolved in DMSO-d_6 and analyzed in the same manner as **3**. HR-MS (ESI): *m/z*: calcd for $C_{22}H_{40}NO_4S$: 414.2672, found:

414.2670 $(M+H)^+$. ^1H NMR (500 MHz, DMSO-d_6, TMS (internal standard)): δ 0.82 (3H, d, $J=7.0$ Hz), 0.83 (3H, t, $J=7.0$ Hz), 1.03–1.10 (1H, m), 1.17–1.32 (18H, overlapped), 1.44–1.53 (2H, m), 1.84 (3H, s), 2.48 (2H, overlapped), 3.12 (1H, dd, $J=8.2$, 13.5 Hz), 3.31 (1H, overlapped), 4.38–4.44 (1H, m), 6.19 (1H, d, $J=15.7$ Hz), 7.76 (1H, d, $J=15.7$ Hz). ^{13}C NMR (125 MHz, DMSO-d_6, TMS (internal standard)): δ 11.1, 19.0, 22.3, 23.8, 26.4, 28.6, 28.7, 28.8 (two carbons), 28.89, 28.94, 29.3, 33.3, 33.6, 35.9, 39.2*, 51.6, 123.1, 146.0, 169.2, 171.3, 196.2 (*signal was detected by DEPT spectra owing to the overlap with the solvent signals).

DLA-derived cysteine

Compound **1** (0.2 mg) was hydrolyzed with 5 N HCl (500 µl) at 105 °C for 1 h. The hydrolysates were concentrated to dryness. To the hydrolysates, water (100 µl) and 1 M $NaHCO_3$ (50 µl) were added, and incubated at 37 °C for 1 h. To the solution (30 µl), 1% D- or L-FDLA/acetone solution (40 µl) was added and incubated at 37 °C for 1.5 h. After the incubation, the reactions were terminated by the addition of 1 N HCl (10 µl). The reactants diluted with 50% aq. methanol were analyzed by LC–HR-MS.

Compound **2** (0.2 mg) was also hydrolyzed, derived with D- or L-FDLA, and analyzed in the same way as described above.

As almost all of the DLA-derived cysteine was observed as DLA-derived cystine and LL-cystine was derived with D- or L-FDLA. In addition, DLA-derived *meso*-cystine standard was made by the method of Kawasaki *et al.* [13]

Detection of the DLA-derived cystine

The DLA-derived cystine were analyzed by LC–HR-MS. LC–HR-MS conditions are described as follows: column, Unison UK-C18, 3µm, 3.0 i.d. × 50 mm (Imtakt); mobile phase, 5 mM aq. ammonium formate in 0.02% formic acid (A): MeCN in 0.02% formic acid (B); gradient rate, A:B (7:3)–A:B (3:7), 10 min; flow rate, 0.6 ml min^{-1}. Retention time of each compounds are as follows: LL-cystine-L-DLA, 6.1 min; LL-cystine-D-DLA, 7.4 min; *meso*-cystine-L-DLA, 5.8 min; *meso*-cystine-D-DLA, 5.8 min; **1**-L-DLA, 6.1 min; **1**-D-DLA, 7.4 min;
2-L-DLA, 6.1 min; **2**-D-DLA, 7.4 min.

VS-G assay

The VS-G assay was established by Ishimoto *et al.*[7] It is a phenotype assay method using a co-culture system of green fluorescent protein (GFP)-labeled HUVECs with fibroblasts.

In brief, GFP-HUVECs were seeded at 7.5×10^3 cells onto the confluent fibroblasts' feeder layers in HuMedia-EG2 (KuRaBo, Tokyo, Japan). After adhesion of GFP-HUVECs to the fibroblasts' layers, assay compounds in assay medium (M199, 0.5% fetal calf serum, 1% penicillin-streptomycin) were added and incubated at 37 °C for 3 days. Cell images were captured by using an In Cell Analyzer 6000 (GE healthcare Japan, Tokyo, Japan) or ImageXpress ULTRA (Molecular Devices, Sunnyvale, CA, USA). The value of area covered by GFP-HUVECs was analyzed using IN Cell Investigator 1.6 (GE healthcare Japan) or MetaXpress (Molecular Devices), and its value was used as *in vitro* activity. Details of the assay method will be described in another report.[7]

CONFLICT OF INTEREST

The authors declare no conflict of interest.

ACKNOWLEDGEMENTS

We are deeply grateful to Mr Akihiro Tamura, Dr Takahiro Yamane and Dr Yuji Kozawa for assistance, and Mr Satoru Ohsuki and Dr Nobuo Machinaga for useful advice.

1 Carmeliet, P. & Jain, R. K. Molecular mechanisms and clinical applications of angiogenesis. *Nature* **473**, 298–307 (2011).
2 Hendrick, A. M., Gibson, M. V. & Kulshreshtha, A. Diabetic retinopathy. *Prim. Care* **42**, 451–464 (2015).
3 Kanazawa, M. *et al.* Inhibition of VEGF signaling pathway attenuates hemorrhage after tPA treatment. *J. Cereb. Blood Flow Metab.* **31**, 1461–1474 (2011).
4 Bates, D. O. Vascular endotherial growth factors and vascular permeability. *Cardiovasc. Res.* **87**, 262–271 (2010).
5 Mathews, M. K., Merges, C., McLeod, D. S. & Lutty, G. A. Vascular endothelial growth factor and vascular permeability changes in human diabetic retinopathy. *Invest. Ophthalmol. Vis. Sci.* **38**, 2729–2741 (1997).
6 Weinberg, D. G. *et al.* Moyamoya disease: a review of histopathology, biochemistry, and genetics. *Neurosurg. Focus* **30**, E20 (2011).
7 Ishimoto, Y. *et al.* A novel natural product-derived compound, vestaine A_1, exerts both pro-angiogenic and anti-permeability activity via a different pathway from VEGF. *Cell. Physiol. and Bio.* (in press).
8 Kim, O. S. *et al.* Introducing EzTaxon-e: a prokaryotic 16S rRNA gene sequence database with phylotypes that represent uncultured species. *Int. J. Syst. Evol. Microbiol.* **62**, 716–721 (2012).
9 Fujii, K., Shimoya, T., Ikai, Y., Oka, H. & Harada, K. Further application of advanced Marfey's method for determination of absolute configuration of primary amino compound. *Tetrahedron Lett.* **39**, 2579–2582 (1998).
10 Bhushan, R. & Brückner, H. Marfey's reagent for chiral amino acid analysis: a review. *Amino Acids* **27**, 231–247 (2004).
11 Jacobson, P. G., Sambandan, T. G. & Morgan, B. Determination of the chirality of cysteines in somatostatin analogs. *J. Chromatogr. A* **816**, 59–64 (1998).
12 Fujii, K. *et al.* Simultaneous detection and determination of the absolute configuration of thiazole-containing amino acids in a peptide. *Tetrahedron* **58**, 6873–6879 (2002).
13 Kawasaki, Y., Nozawa, Y. & Harada, K. Elution behavior of diaminopimelic acid and related diamino acids using the advanced Marfey's method. *J. Chromatogr. A* **1160**, 246–253 (2007).